Virus Research 260 (2019) 102–113

Contents lists available at ScienceDirect

Virus Research

journal homepage: www.elsevier.com/locate/virusres

Virus- and cell type-specific effects in orthohantavirus infection

Stefan Hägele[a,1], Alexander Müller[a,1], Christian Nusshag[a], Jochen Reiser[b], Martin Zeier[a], Ellen Krautkrämer[a,*]

[a] Department of Nephrology, University of Heidelberg, Heidelberg, Germany
[b] Department of Medicine, Rush University, Medical Center, Chicago, IL, USA

ARTICLE INFO

Keywords:
Orthohantavirus
Puumala virus
Hantaan virus
Cytoskeleton
Kidney
Release

ABSTRACT

Orthohantaviruses Hantaan (HTNV) and Puumala (PUUV) virus cause hemorrhagic fever with renal syndrome (HFRS), that is characterized by acute renal failure with often massive proteinuria and by morphological changes of the tubular and glomerular apparatus. Orthohantaviral N protein is found in renal cells and plays a key role in replication. However, the replication in human renal cells is not well characterized.

Therefore, we examined the orthohantaviral infection in different human renal cells. Differences in localization of N protein, release of particles, and modulation of the actin cytoskeleton between both virus species are observed in human renal cells. A substantial portion of HTNV N protein demonstrates a filamentous pattern in addition to the typical punctate pattern. Release of HTNV depends on an intact actin and microtubule cytoskeleton. In contrast, PUUV N protein is generally localized in a punctate pattern and release of PUUV does not require an intact actin cytoskeleton. Infection of podocytes results in cytoskeletal rearrangements that are more pronounced for HTNV. Analyzing Vero E6 cells revealed differences compared to human renal cells. The pattern of N proteins is strictly punctate, release does not depend on an intact actin cytoskeleton and cytoskeletal rearrangements are not present. No virus-specific variations between HTNV and PUUV are observed in Vero E6 cells.

Using human renal cells as cell culture model for orthohantavirus infection demonstrates virus-specific differences and orthohantavirus-induced cytoskeletal rearrangements that are not observed in Vero E6 cells. Therefore, the choice of an appropriate cell culture system is a prerequisite to study orthohantavirus pathogenicity.

1. Introduction

Orthohantaviruses cause hantaviral cardio-pulmonary syndrome (HCPS) or hemorrhagic fever with renal syndrome (HFRS) characterized by a predominant pulmonary or renal involvement, respectively (Vaheri et al., 2013). The clinical course of orthohantavirus infections has a wide spectrum of severity and symptoms and varies enormously between species despite sharing high levels of genetic homology. The underlying molecular mechanisms are not completely understood. A plethora of different cell types and cell lines have been described to be susceptible to orthohantavirus infection *in vitro* (Guhl et al., 2010; Higa et al., 2012; Temonen et al., 1993). Analyzing the orthohantaviral replication cycle *in vitro*, revealed differences for the entry and regulation of cellular response between pathogenic and non-pathogenic species, the release of New and Old World orthohantaviruses and even orthohantavirus genotypes differ in the induction of gene expression profiles (Gavrilovskaya et al., 1999; Geimonen et al., 2002; Ramanathan and Jonsson, 2008; Shin et al., 2013; Witkowski et al., 2016). However, it is not clear which mechanisms account for the variance in organ manifestation and severity of orthohantavirus infection *in vivo*.

Infections with the pathogenic Old World orthohantavirus species Hantaan (HTNV) and Puumala (PUUV) virus cause HFRS. Renal involvement predominates in most cases leading to acute renal failure with often massive proteinuria (Krautkrämer and Zeier, 2014). However, the clinical course of PUUV infections is milder than of HTNV infection. As mentioned before, orthohantaviruses share high sequence similarity and the molecular and cellular factors that determine species-specific pathogenicity and organ tropism have not been identified so far. The differences in severity and organ manifestation strongly suggest that virus- and cell type-specific characteristics in the orthohantaviral replication cycle exist. HTNV and PUUV are pathogenic species and probably enter their target cells *via* the same entry mechanism using

* Corresponding author at: Department of Nephrology, University of Heidelberg, Im Neuenheimer Feld 162, 69120 Heidelberg, Germany.
E-mail address: ellen.krautkraemer@med.uni-heidelberg.de (E. Krautkrämer).
[1] Contributed equally.

https://doi.org/10.1016/j.virusres.2018.11.015
Received 26 July 2018; Received in revised form 15 November 2018; Accepted 29 November 2018
Available online 30 November 2018

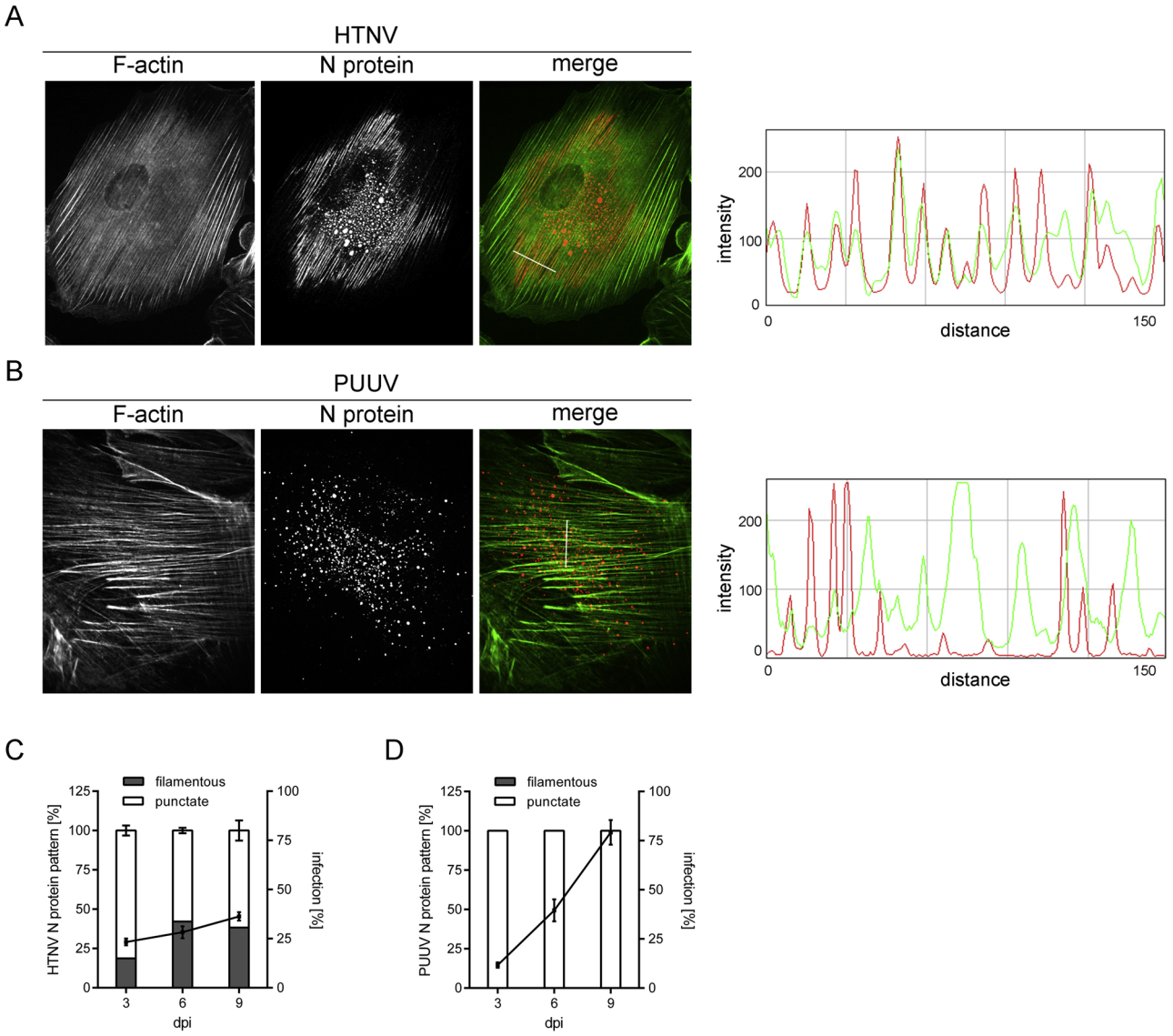

Fig. 1. Localization of orthohantaviral N protein in HREpCs. HREpCs were infected with HTNV (A) or PUUV (B) and analyzed for N protein and F-actin by confocal microscopy on day nine post infection (dpi). Histograms show the fluorescence intensity profiles of N protein and F-actin along the indicated lines. Cells were imaged at a magnification of ×1000. (C and D) HREpCs were analyzed for HTNV (C) and PUUV (D) infection (right y-axis) and localization pattern of N protein (left y-axis) over time. The localization of N protein was analyzed in 100 cells in each experiment. Three independent experiments were performed. Shown is mean ± SD.

integrin β_3 and CD55 as receptors (Gavrilovskaya et al., 1999; Krautkrämer and Zeier, 2008). Both virus species infect renal cell types and disturb their cell-to-cell contacts (Krautkrämer et al., 2011). Therefore, differences in post-entry steps in the viral replication cycle of HTNV and PUUV seem to be responsible for the variation in the clinical picture. Replication, assembly and release of new particles require interaction with the host cell machinery, reorganization of the cytoskeleton and interfere with proper host cell signaling. The orthohantaviral N protein plays a crucial role in viral replication by modulation of translation, signaling processes and by defining the localization of viral components during assembly of new particles (Reuter and Krüger, 2018). Studying orthohantaviral replication cycle *in vivo* is hampered by the lack of a suitable small animal model and the analysis *in vitro* requires an adequate cell culture model. Vero E6 cells, an epithelial cell line derived from African Green Monkey kidney, are often used in Old World orthohantavirus studies. The lack of an intact interferon system in Vero E6 cells favors these cells for virus propagation but may be of disadvantage in studying pathogenesis of orthohantavirus infection, because the replication cycle may not reflect the situation in target cells (Emeny and Morgan, 1979; Prescott et al., 2017).

Therefore, we analyzed and compared infection with PUUV and HTNV in human primary renal cells, a human podocyte cell line, and Vero E6 cells.

2. Materials and methods

2.1. Cells and viruses

Human renal epithelial cells (HREpCs) were cultured in renal epithelial cell growth medium-2 (Promocell). Primary podocytes (Lonza)

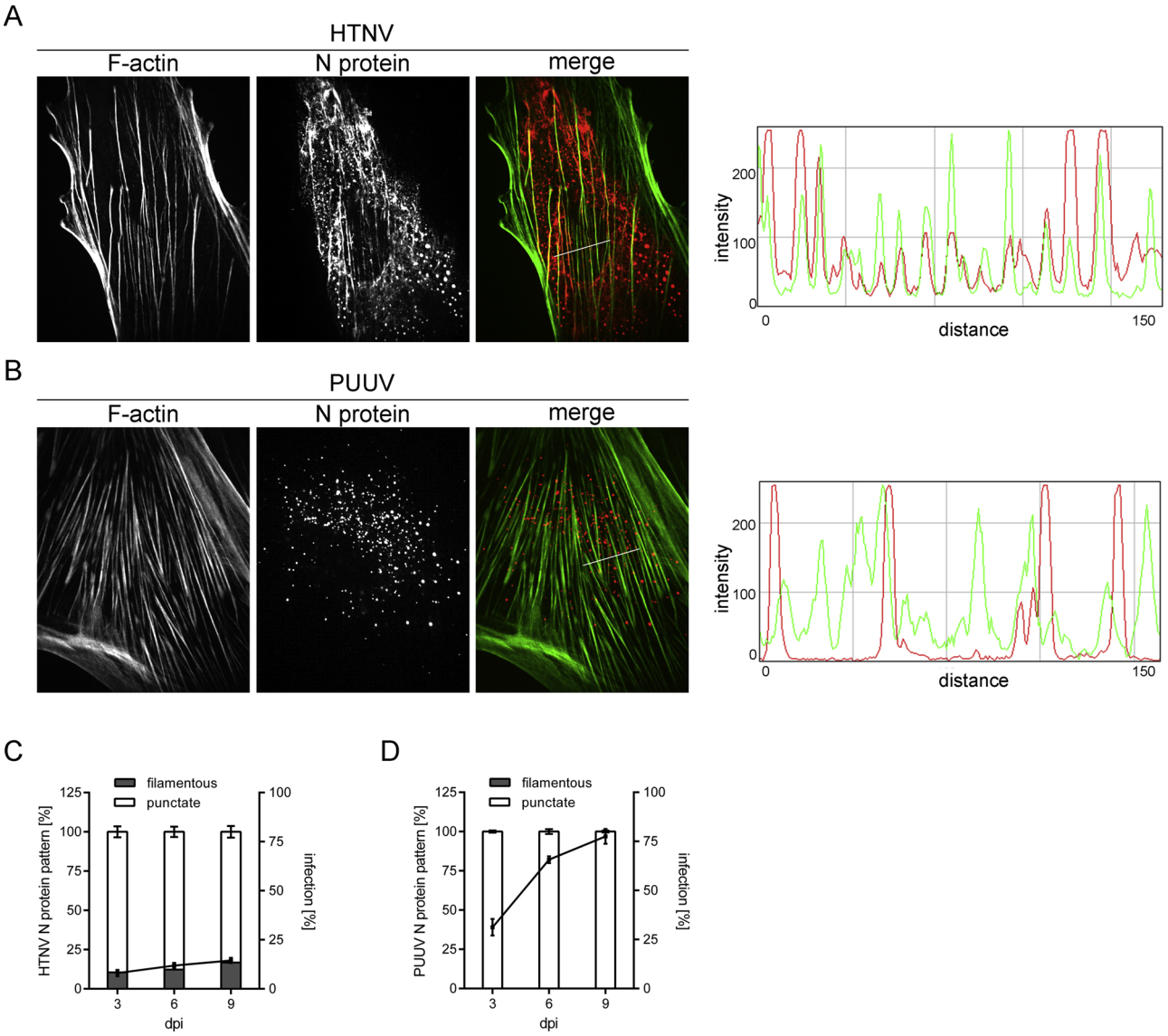

Fig. 2. Localization of orthohantaviral N protein in human primary podocytes. Podocytes were infected with HTNV (A) or PUUV (B) and analyzed for N protein and F-actin by confocal microscopy on day nine after infection. Histograms show the fluorescence intensity profiles of N protein and F-actin along the indicated lines. Cells were imaged at a magnification of ×1000. (C and D) Podocytes were analyzed for HTNV (C) and PUUV (D) infection (right y-axis) and localization pattern of N protein (left y-axis) over time. The localization of N protein was analyzed in 100 cells in each experiment. Three independent experiments were performed. Shown is mean ± SD.

were maintained in RPMI medium supplemented with 10% FCS and 1% Insulin-Transferrin-Selenium (ITS) (Capricorn). Primary cells were only used for experiments from passages two to six. Vero E6 cells were maintained in DMEM supplemented with 10% FCS. The human podocyte cell line was derived from human normal podocytes conditionally transformed with a temperature-sensitive mutant of the simian virus 40 (SV40) large T antigen (Saleem et al., 2002). For proliferation, cells were cultured in RPMI medium supplemented with 10% FCS, 1% ITS, and 5000 U interferon-gamma (IFN-γ) at 33 °C. After transfer to 37 °C for 14 days in medium without IFN-γ, podocytes undergo growth arrest and express markers of differentiation. Expression of the podocyte-specific marker synaptopodin was routinely controlled. Experiments were performed with non-proliferating and differentiated podocytes. Orthohantavirus species Hantaan virus strain 76–118 (HTNV) and Puumala virus strain Vranica (PUUV) were propagated on Vero E6 cells. For infection, cells were incubated with viral inocula at an MOI of 0.1 that was determined by titration on Vero E6 cells. Medium was replaced after six hours and a triple wash. Viability of cells was not affected by infection. The number of viable cells was determined by measuring the amount of ATP using CellTiter-Glo luminescent cell viability assay (Promega). Work with PUUV and HTNV was carried out in biosafety level 2 and 3 containment facilities, respectively.

2.2. Immunofluorescence

Cells grown on coverslips were fixed with 3% paraformaldehyde and stained with primary and fluorescently-labeled secondary antibodies. The following antibodies were used: Mouse anti-tubulin-α

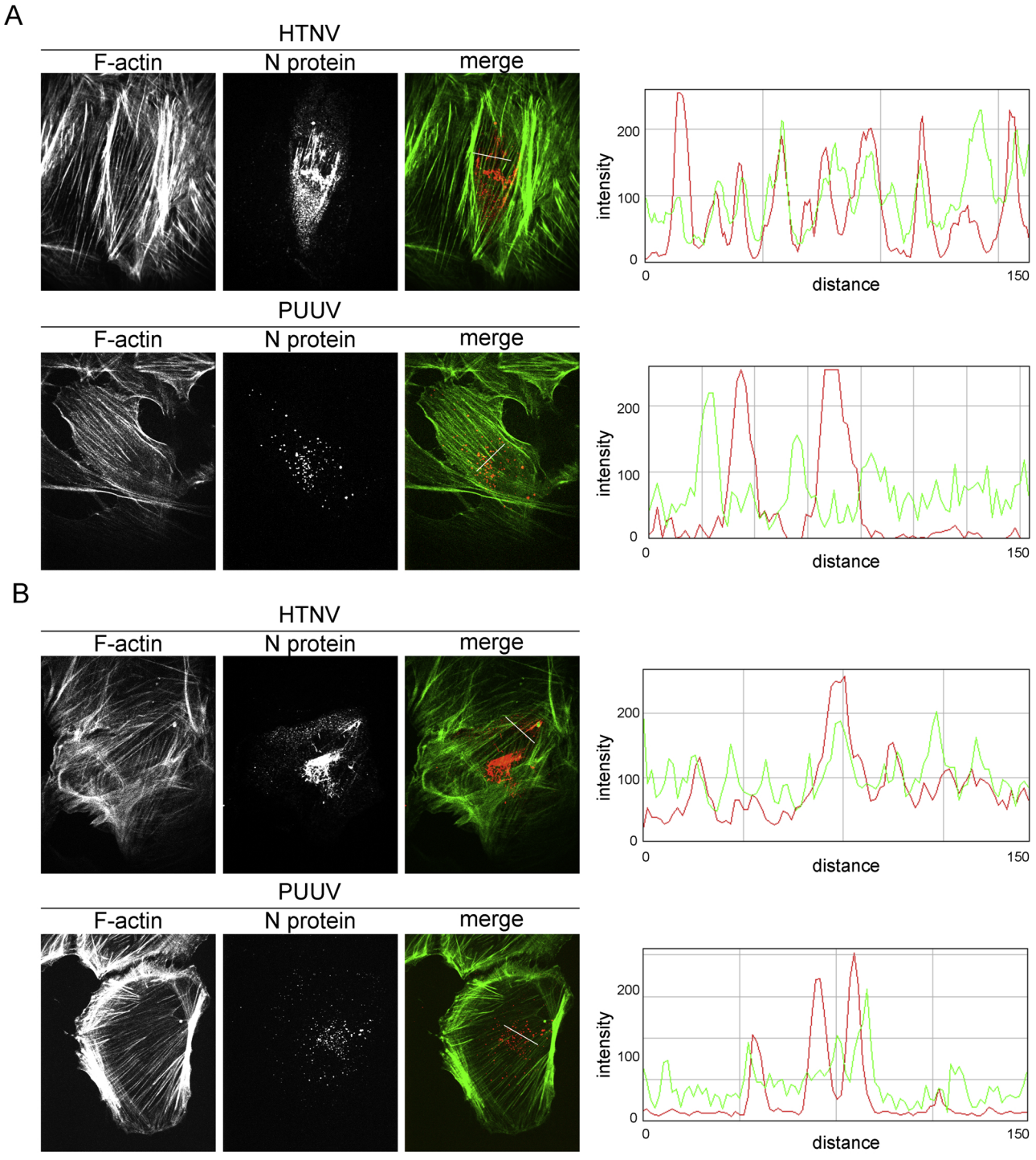

(caption on next page)

Fig. 3. Infection of HREpCs and human primary podocytes derived from second donors with orthohantaviruses HTNV and PUUV. HREpCs (A) and primary podocytes (B) were infected with HTNV or PUUV and analyzed for N protein and F-actin by confocal microscopy on day nine after infection. Histograms show the fluorescence intensity profiles of N protein and F-actin along the indicated lines. Cells were imaged at a magnification of ×1000. (C) HREpCs and podocytes were analyzed for HTNV and PUUV infection (right y-axis) and localization pattern of N protein (left y-axis) on day nine post infection. The localization of N protein was analyzed in 100 cells in each experiment. Three independent experiments were performed. Shown is mean ± SD.

(DM1 A, Sigma-Aldrich), mouse anti-nucleocapsid (N) protein PUUV (A1C5, Progen), mouse anti-N protein HTNV (B5D9, Progen), rabbit anti-N protein PUUV and HTNV. Cell nuclei were stained by Hoechst 33,342 (Invitrogen) and F-actin by Alexa Fluor 488 phalloidin (Invitrogen). Images were taken using an Axiocam 506 mono camera attached to an Axio Observer.D1 inverted microscope (Carl Zeiss). Confocal microscopy analysis was performed by a Nikon TE-2000 inverted microscope with a Hamamatsu C9100-02 EMCCD camera (Nikon).

2.3. Treatment with cytochalasin D and nocodazole

In each experiment, cells were inoculated with orthohantaviruses in triplicates. After washing, cells were infected for six days. Cells were washed three times with medium to remove remaining viral particles and incubated with fresh medium for four hours as reference for viral release. For treatment, cells were washed and incubated with fresh medium for four hours supplemented with either DMSO solvent control or cytoskeletal depolymerization inhibitors. Podocytes were incubated with 1 µM cytochalasin D (Merck) and 10 µM nocodazole (Merck) whereas Vero E6 cells were treated with 8 µM cytochalasin D and 10 µM nocodazole. The chosen concentrations did not affect cell viability as determined by CellTiter-Glo luminescent cell viability assay (Promega). Again, for recovery, cells were washed and incubated with normal medium for another four hours. Cell-free supernatants were harvested after reference, treatment, and recovery phase. The amount of infectious viral particles in the supernatants was determined by In-Cell Western assay and the amount of infectious viral particles in the reference sample was set to 100%.

2.4. In-Cell Western assay

To measure release of infectious particles, equal volumes of virus-containing supernatants were added in triplicates to Vero E6 cells grown in 96-well plates. To quantify infection, cells were fixed at two days post infection and subjected to In-Cell Western assay. Cells were permeabilized and stained for N protein and with the respective near-infrared fluorescence-conjugated secondary antibodies. Infection was normalized to cell number by staining of nuclei with DRAQ5/Sapphire according to the manufacturer's protocol. Plates were scanned with Odyssey Imaging System (Li-Cor) and integrated fluorescence intensities of N protein and nuclei stainings were determined using the Image Studio software with the In-Cell Western module.

2.5. Quantification of F-/G-actin ratio

Ratios of globular (G) and filamentous (F) actin were determined according to the manufacturer's protocol of the G-actin/F-actin *in vivo* Assay Kit (Cytoskeleton, Inc.). Briefly, uninfected and infected cells were lysed in a detergent-based buffer that stabilizes pools of F- and G-actin. F- and G-actin were separated by ultracentrifugation. F-actin was found in the insoluble fraction whereas G-actin was detected in the supernatant. Treatment of cells with the actin-polymerizing drug phalloidin resulted in the accumulation of actin in the insoluble fraction and served as control for the fractionation procedure. Actin content of fractions was analyzed by Western blot using the following antibodies: Rabbit anti-actin (Cytoskeleton, Inc.), rabbit anti-HTNV N protein, rabbit anti-PUUV N protein and near-infrared fluorescently-labeled secondary antibodies. The membrane was scanned by the Odyssey infrared imaging system. Quantitative image analysis was performed by using the Image Studio software.

2.6. Statistical analysis

Data were analyzed using Prism 5.0 (GraphPad Software Inc.). Normal distribution was tested with the Kolmogorov-Smirnov test. Values of two groups were compared using two-tailed Student's t-test. P values of < 0.05 were considered significant. $^{*}P < 0.05$; $^{**}P < 0.005$; $^{***}P < 0.0005$; $^{****}P < 0.0001$; ns: not significant.

3. Results

3.1. Localization of orthohantaviral N protein in human primary renal cells

To examine the localization of orthohantaviral N proteins, we stained HTNV- and PUUV-infected human primary renal cells for the cytoskeletal component F-actin together with N protein (Figs. 1 and 2). N proteins of HTNV and PUUV in infected HREpCs differed in their localization (Figs. 1A and B). HTNV N protein was localized in punctate and filamentous pattern whereas PUUV N protein was found exclusively in a punctate pattern. HTNV N protein appearing in a filamentous pattern partially co-localized with actin stress fibers in HREpCs (Fig. 1A). The percentage of infected HREpCs showing a filamentous pattern of HTNV N protein increased over time (Fig. 1C). A similar pattern was observed in infected primary human podocytes (Fig. 2). As observed for HREpCs, HTNV N protein showed a filamentous and punctate distribution, whereas the filamentous pattern was absent in PUUV-infected podocytes (Fig. 2A and B). After nine days of infection, about 75% of HREpCs and primary podocytes were infected with PUUV (Figs. 1D and 2 D). In contrast, only 36.33% of HREpCs and 14.48% of primary podocytes were positive for HTNV N protein on day nine post infection (Figs. 1C and 2 C). To test susceptibility and N protein localization for possible donor-specific effects, we repeated the analysis with cells derived from other donors (Fig. 3). HREpCs were susceptible to infection with HTNV (56.37%) and PUUV (83.25%). The primary podocytes were also infected with HTNV (9.80%) and PUUV (75.85%). The filamentous pattern of HTNV N protein localization was observed in 22.24% of HREpCs and 31.39% of primary podocytes. Cells infected with PUUV did not exhibit a filamentous localization of N protein (Fig. 3C).

3.2. Localization of N protein in renal cell lines

We compared the localization of HTNV N protein in primary renal cells with the localization in infected cell lines: a human podocyte cell line and Vero E6 cells, an epithelial cell line derived from African Green Monkey kidney and widely used in orthohantavirus studies (Figs. 4 and 5). The staining pattern of HTNV N protein in Vero E6 cells and human renal cells differed enormously. Infection of the podocyte cell line revealed a filamentous localization of HTNV N protein and a partial co-

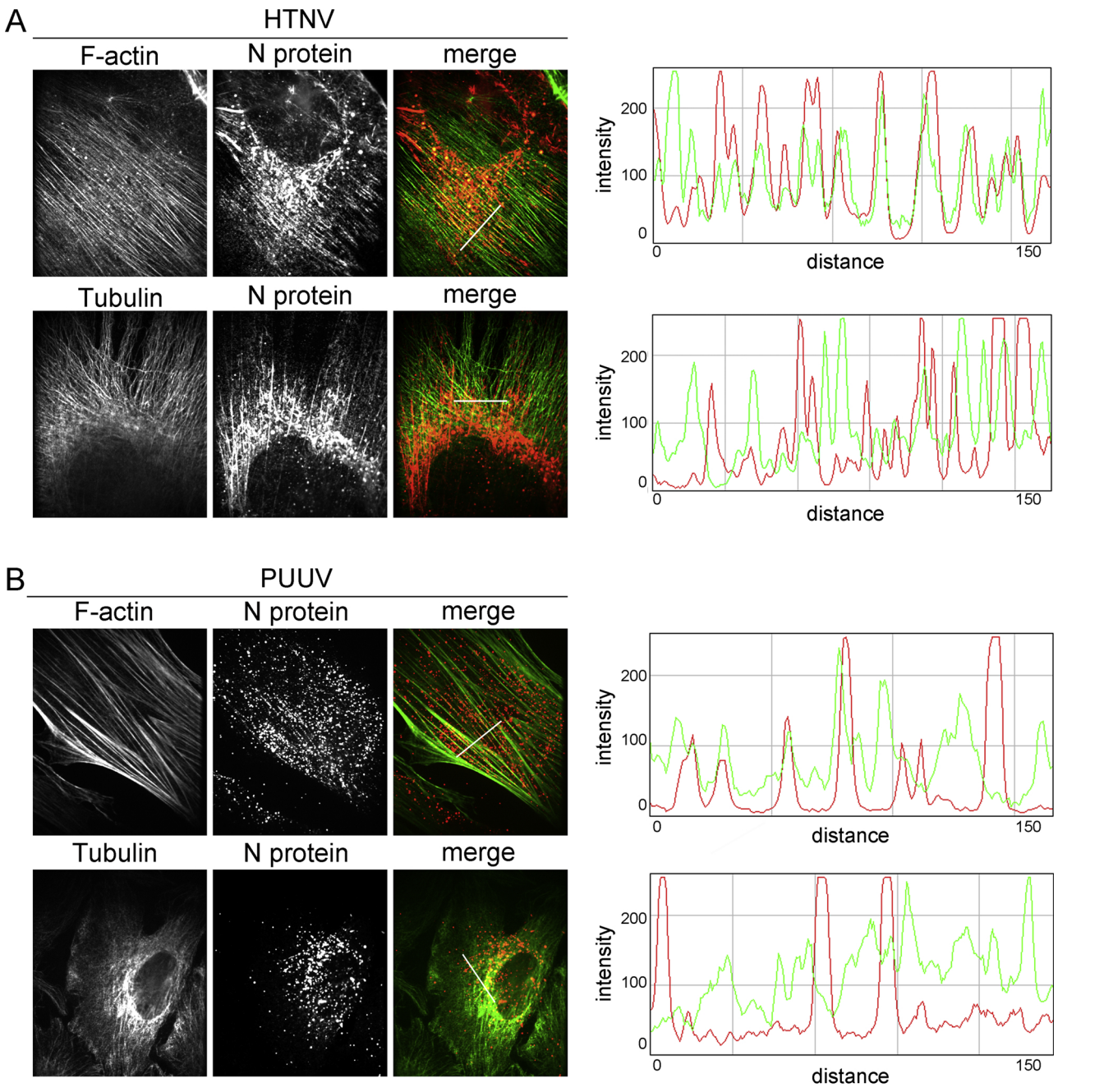

(caption on next page)

Fig. 4. Localization of orthohantaviral N protein in a podocyte cell line. Podocytes were infected with HTNV (A) or PUUV (B) and analyzed for N protein, F-actin, and tubulin localization by confocal microscopy on day six after infection. Histograms show the fluorescence intensity profiles of F-actin, tubulin, and N protein staining along the indicated lines. Cells were imaged at a magnification of ×1000. (C) HTNV- or (D) PUUV-infected podocytes were analyzed for the localization pattern of N protein and number of infected cells over time. The localization of N protein was analyzed in 100 cells in each experiment. Data were obtained from three independent experiments. Shown is mean ± SD.

localization with F-actin stress fibers as observed for human primary cells (Fig. 4). Vero E6 cells exhibited a more punctate pattern of N protein without co-localization with F-actin and lacked the filamentous structures detected in human renal cells (Fig. 5). In contrast to primary cells, single cells of the podocyte cell line exhibit a co-localization of PUUV N protein with F-actin stress fibers (Fig. 4B).

To exclude that the observed differences between Vero E6 cells and human renal cells in N protein localization were due to variances in the replication kinetics, we examined the localization of N protein in Vero E6 cells over time (Fig. 5C). HTNV N protein in Vero E6 cells was strictly localized in a punctate pattern, whereas the number of human renal cells showing a filamentous pattern of N protein increased over time (compare Fig. 5C with Figs. 1C, 2 C, and 4 C).

Together, the localization of HTNV N protein observed in human cells differed from the pattern in Vero E6 cells. In addition, the podocyte cell line exhibited a higher susceptibility to HTNV infection than human primary podocytes.

3.3. Role of the cytoskeleton in N protein localization

To analyze the involvement of cytoskeletal components in the localization of orthohantaviral N protein, we treated infected cells of the podocyte cell line with cytochalasin D or nocodazole that inhibit the polymerization of actin and tubulin, respectively (Fig. 6). Disturbance of the actin cytoskeleton resulted in the redistribution of HTNV N protein in the perinuclear region with a punctate pattern. In contrast, nocodazole did not cause any effect on N protein localization. The specific localization of N protein was completely restored after washout of cytochalasin D indicating that an intact actin cytoskeleton is a prerequisite for the filamentous pattern of orthohantaviral N protein (Fig. 6A and B).

As observed for HTNV N protein, the filamentous pattern of PUUV N protein localization observed in some cells disappeared after the disruption of actin filaments by treatment of podocytes with cytochalasin D and was restored after removal of the drug. No changes in PUUV N protein pattern were detected in podocytes treated with nocodazole (Fig. 6C and D).

3.4. Release of orthohantaviral particles

To examine the role of the cytoskeleton in orthohantaviral replication, we analyzed the effects of inhibitors of actin and microtubule polymerization on the release of particles (Fig. 7). Vero E6 cells were incubated with cytochalasin D or nocodazole to depolymerize actin and microtubules, respectively (Fig. 7A). Treatment of infected Vero E6 cells with nocodazole revealed a serious reduction of infectious HTNV and PUUV particles whereas cytochalasin exerted no effect on viral release. The amount of HTNV and PUUV virions in the supernatant of nocodazaole-treated infected podocytes was also decreased compared to untreated cells (Fig. 7B). However, the inhibition was less pronounced than observed in Vero E6 cells treated with nocodazole. In addition, the treatment with cytochalasin D reduced the release of HTNV virions by half. In contrast, actin depolymerization did not influence the release of PUUV virions. The observed effects of drug treatment were completely reverted after four hours of recovery.

These results demonstrate that orthohantaviral release depends on cytoskeletal integrity in a virus- and cell type-specific manner.

3.5. Effects of orthohantavirus infection on actin cytoskeleton

Viral release, cellular morphology and function strongly depend on the integrity of the cytoskeleton. Therefore, we analyzed the actin cytoskeleton in infected and uninfected cells by quantifying the amount of F- and G-actin (Fig. 8). No effect on cytoskeletal organization was observed in orthohantavirus infected Vero E6 cells (Fig. 8A). In contrast, a significant rearrangement was detected in infected podocytes (Fig. 8B). Compared to uninfected podocytes, the abundance of actin in the insoluble fraction of HTNV-infected cells was decreased and the ratio of F- and G-actin was significantly altered (0.45 ± 0.09 *vs.* 1.00 ± 0.14, $P = 0.0045$). The majority of N protein was found in the insoluble fraction. As observed for HTNV, the cytoskeletal organization of podocytes was also influenced by PUUV resulting in the reduction of F-/G-actin ratio to 0.67 ± 0.12 *vs.* 1.00 ± 0.11; ($P = 0.0245$) in uninfected podocytes.

4. Discussion

Infection with HTNV or PUUV is characterized by massive renal involvement. Glomerular and tubular cells of the kidney represent target cells of orthohantaviruses. Infection of renal cells with PUUV disturbs the integrity of cell-to cell contacts and interferes with barrier function (Boehlke et al., 2014; Krautkrämer et al., 2011). However, the severity of the clinical picture varies enormously between the two species. Modulations of signaling pathways and replication kinetics may influence the clinical course (Korva et al., 2013; Saksida et al., 2008; Yi et al., 2013). However, the underlying molecular mechanisms and effects in target cells are not completely understood. Using human renal cells, we demonstrate that HTNV and PUUV show differences in the localization of N protein, the release of viral particles, and modulation of the cytoskeleton. Interestingly, the replication cycle in Vero E6 cells differs from the infection in human renal cells.

The observed virus- and cell-type specific effects raise the question of an adequate cell culture model of orthohantavirus infection. Human primary tubular epithelial cells and podocytes are permissive for PUUV and HTNV infection *in vitro*. However, the infection rates for HTNV are low and the uninfected cell population hampers the analysis of orthohantavirus-induced effects. In addition, donor-specific effects and dedifferentiation of primary cells during experiments make the use as cell culture model more difficult. In contrast, Vero E6 cells and the podocyte cell line demonstrate a high rate of PUUV and HTNV infection. However, the localization of N protein, release, and functional consequences in infected Vero E6 cells did not correspond to the orthohantaviral replication in primary renal cells. The lack of an intact interferon system or the adaptation of orthohantaviruses to Vero E6 cell culture propagation may account for these differences (Lundkvist et al., 1997; Nemirov et al., 2003). The role of filamentous localization of HTNV N protein and its absence in Vero E6 cells requires further investigation. Only an amount of cells exhibit this pattern, but the process of filamentous N protein localization is dynamic and depends on an intact actin cytoskeleton as shown by treatment with cytochalasin D.

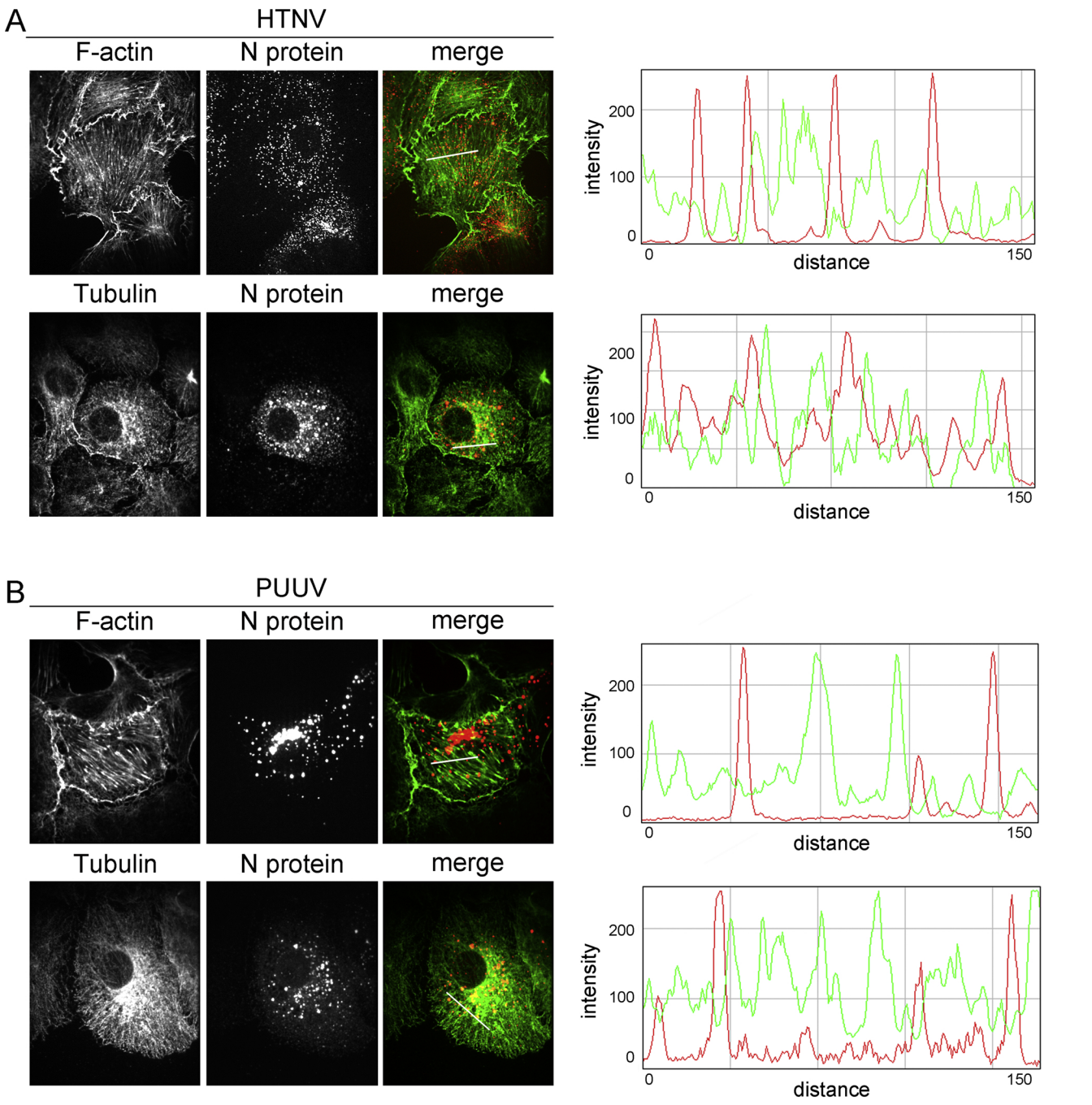

(caption on next page)

Fig. 5. Localization of orthohantaviral N protein in Vero E6 cells. Cells were infected with HTNV (A) or PUUV (B) and analyzed for N protein, F-actin, and tubulin localization by confocal microscopy on day six after infection. Histograms show the fluorescence intensity profiles of F-actin, tubulin, and N protein staining along the indicated lines. Cells were imaged at a magnification of ×1000. (C) HTNV- or (D) PUUV-infected Vero E6 cells were analyzed for the localization pattern of N protein and number of infected cells over time. The localization of N protein was analyzed in 100 cells in each experiment. Data were obtained from three independent experiments. Shown is mean ± SD.

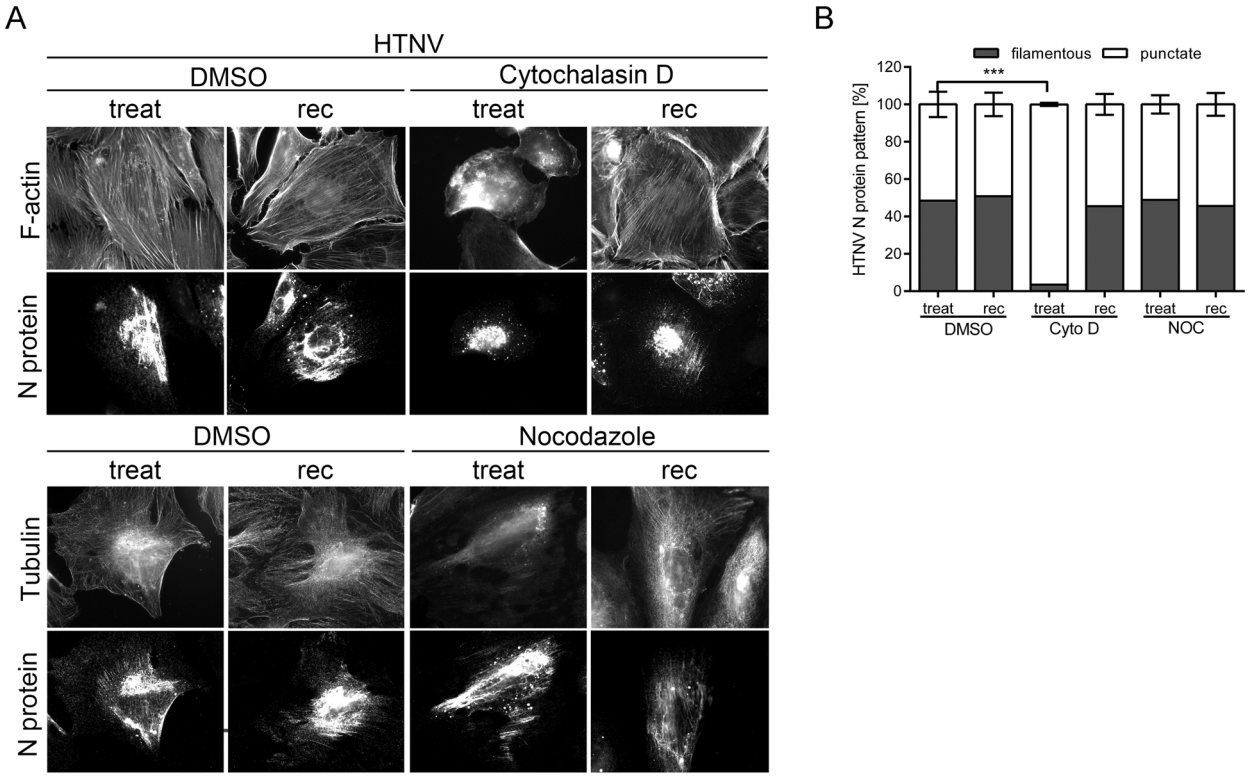

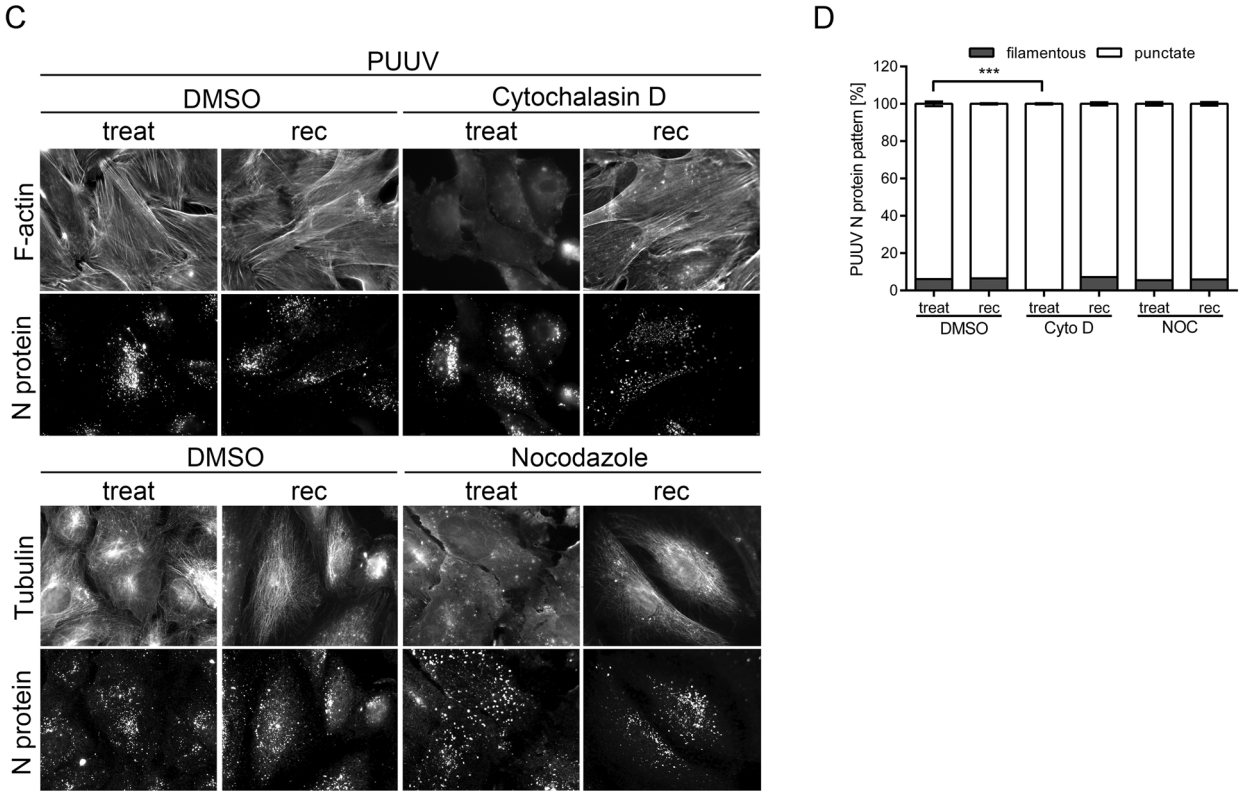

Fig. 6. Localization of N protein after drug treatment. Cells of the podocyte cell line were infected with HTNV (A) or PUUV (C) and treated with solvent control (DMSO), cytochalasin D (Cyto D), or nocodazole (NOC) on day six post infection. Localization of N protein, F-actin, and tubulin was analyzed after drug treatment (treat) and after recovery (rec) by fluorescence microscopy. Cells were imaged at a magnification of ×1000. (B and D) The localization pattern of HTNV (B) and PUUV (D) N protein of 100 DMSO- and drug-treated infected podocytes was quantified in each experiment. Three independent experiments were performed. Shown is mean ± SD.

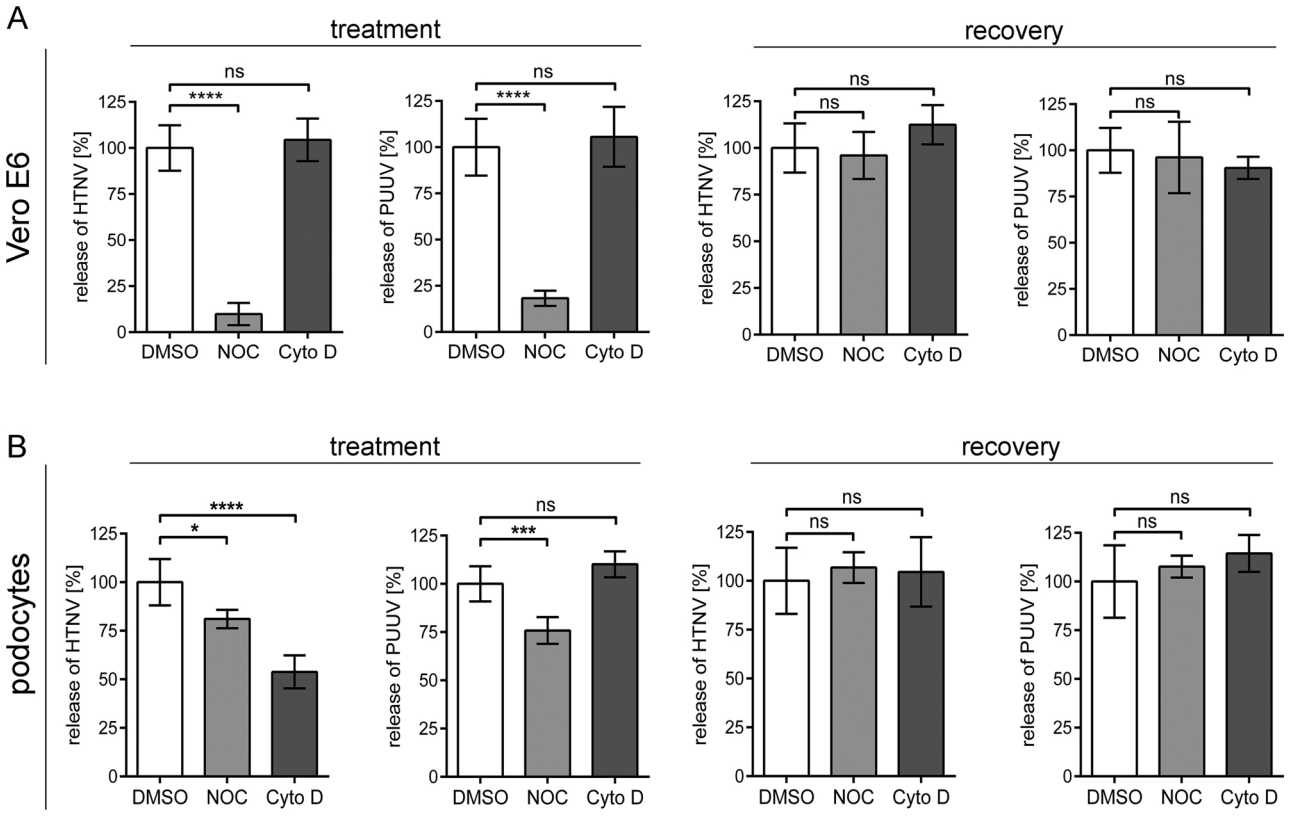

Fig. 7. Release of orthohantaviruses from Vero E6 and podocyte cell line. Cells were infected with HTNV or PUUV and treated with DMSO, Cyto D, or NOC for four hours on day six post infection. (A) Quantification of infectious particles in the supernatants of treated Vero E6 cells by In-Cell Western (treatment). After drug treatment, Vero E6 cells were washed, incubated for another four hours with fresh media and infectious particles in the supernatant were quantified (recovery). Three independent experiments were performed in triplicates. Shown is mean ± SD. (B) Infectious particles in the supernatant of infected podocytes were quantified as described in (A) for Vero E6 cells.

Since orthohantaviral N protein plays a crucial role in the localization of viral components and release of novel particles, the filamentous localization may be important for these functions in human renal cells (Hepojoki et al., 2010; Li et al., 2010; Shimizu et al., 2013). The impaired release of HTNV particles after cytochalasin D treatment may be a hint for a specific interplay of actin and N protein in viral assembly or release in renal cells. Orthohantaviruses infect highly-differentiated, polarized epithelial and endothelial cells. The modulation of the cytoskeleton may also be important for the egress from polarized monolayers as shown for other viruses. Viral release can occur bidirectionally or predominantly from the apical or basolateral surface of polarized cells. The specific release requires the correct transport of viral particles to the apical or basolateral side. It was shown for Junin virus that disruption of the microtubule network results in the non-polarized release of Junin virus despite the monolayers were still effective permeability barriers (Cordo et al., 2005). To study if orthohantaviruses exhibit a cell-type specific polarized release that depends on different cytoskeletal components would improve the understanding of orthohantaviral dissemination and spread of infection.

Our results demonstrate that orthohantavirus infection exerts virus- and cell-type specific characteristics and consequences in renal cells. These effects may contribute to the clinical picture of orthohantavirus infection. Proper renal function depends on glomerular and tubular cells and both structures are affected in orthohantavirus-induced acute renal injury (Boehlke et al., 2014; Ferluga and Vizjak, 2008; Krautkrämer et al., 2011; Mantula et al., 2017; Mustonen et al., 1994; Temonen et al., 1993). Podocyte foot process effacement was observed in renal biopsies from orthohantavirus infected patients (Boehlke et al., 2014). Since disturbance of the podocyte actin cytoskeleton results in foot process effacement leading to kidney dysfunction, the orthohantavirus-induced modulation of the cytoskeleton may contribute to the morphological change of podocyte architecture (Welsh and Saleem, 2011). The cytoskeletal rearrangement is less pronounced in PUUV-infected than in HTNV-infected podocytes. This may indicate a possible association between the observed effect and the milder clinical course of PUUV infection in patients. The study of the cytoskeletal consequences of infection with virus species or genotypes with different pathogenicity will provide a more detailed insight in this possible mechanism of orthohantaviral pathogenesis. In addition, it would be of interest to analyze possible adaptations of viruses to renal cells. The amino acid sequence of N protein is preserved during virus propagation in cell culture, whereas the non-coding sequence of PUUV S segment shows alterations during cell culture passaging (Lundkvist et al., 1997). Such alterations may play a role during replication in renal target cells.

The use of human primary cells derived from target organ kidney or corresponding cell lines will be helpful to identify functional consequences of renal infection and will provide useful insights in the replication cycle and renal pathomechanisms of orthohantaviruses.

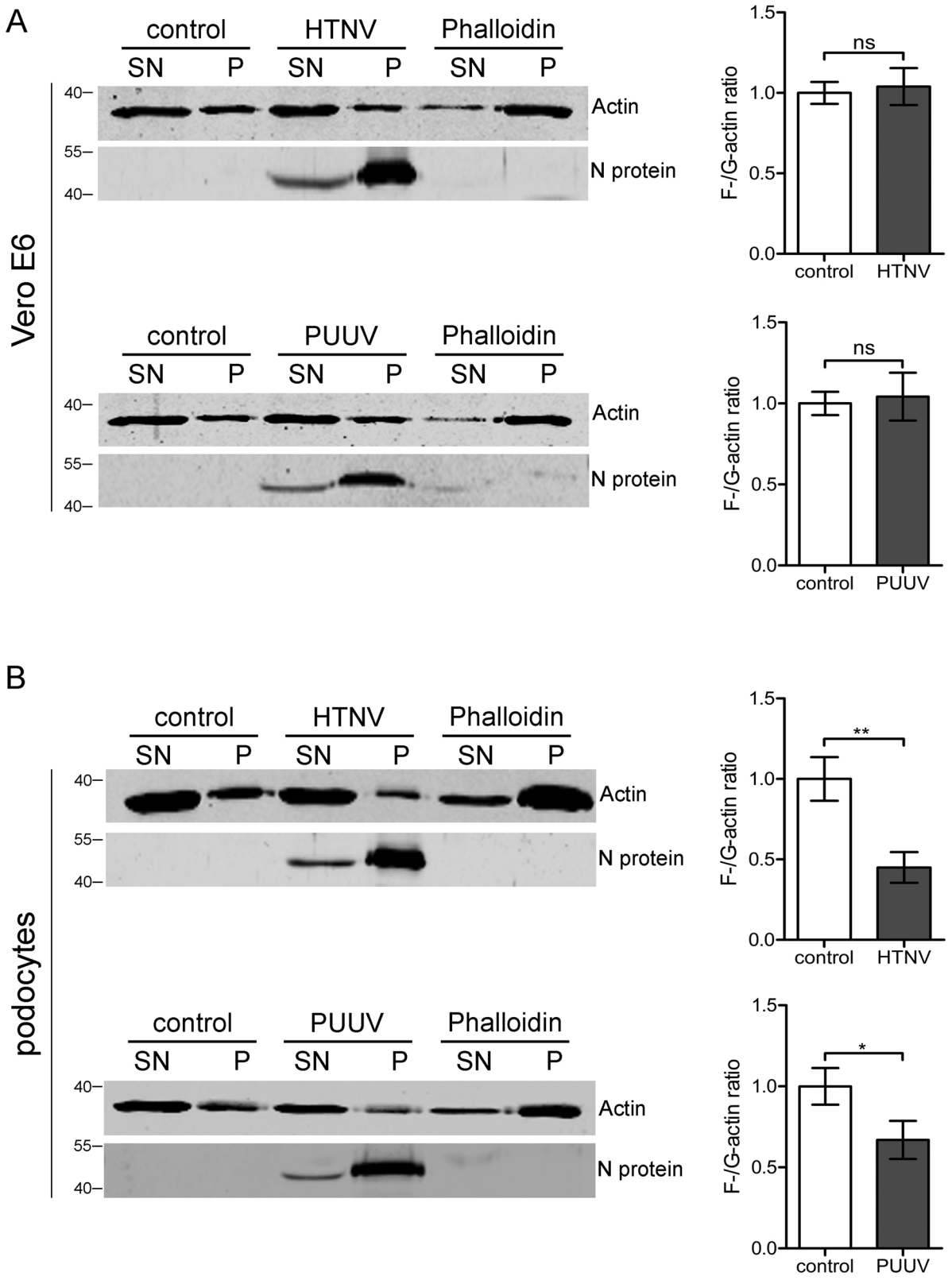

Fig. 8. Cytoskeletal organization in orthohantavirus infected Vero E6 and podocyte cell line. (A) Vero E6 cells were infected with HTNV or PUUV and subjected to fractionation. Fractionated cellular lysates (SN: supernatant, P: pellet) of uninfected, HTNV-infected, and phalloidin-treated cells were analyzed for actin and N protein by Western blot. Shown is one representative Western blot of three independent experiments. Relative F-/G-actin ratio was quantified by measuring band intensities from Western blot. The ratio of uninfected cells was set to 1. Shown is mean ± SD. (B) Cytoskeletal organization of podocytes infected with HTNV or PUUV was analyzed as described in (A) for Vero E6 cells.

Ethical approval

All procedures performed in studies involving human participants were in accordance with the ethical standards of the institutional and national research committee and with the 1964 Helsinki declaration and its later amendments or comparable ethical standards.

Funding

This research did not receive any specific grant from funding agencies in the public, commercial, or not-for-profit sectors.

Declarations of interest

The authors declare that they have no competing interests.

Acknowledgments

We thank Ulrike Engel and Christian Ackermann for the support in microscopy at the Nikon Imaging Center (Heidelberg).

References

Boehlke, C., Hartleben, B., Huber, T.B., Hopfer, H., Walz, G., Neumann-Haefelin, E., 2014. Hantavirus infection with severe proteinuria and podocyte foot-process effacement. Am. J. Kidney Dis. 64 (3), 452–456.

Cordo, S.M., Cesio y Acuna, M., Candurra, N.A., 2005. Polarized entry and release of Junin virus, a New World arenavirus. J. Gen. Virol. 86 (Pt 5), 1475–1479.

Emeny, J.M., Morgan, M.J., 1979. Regulation of the interferon system: evidence that Vero cells have a genetic defect in interferon production. J. Gen. Virol. 43 (1), 247–252.

Ferluga, D., Vizjak, A., 2008. Hantavirus nephropathy. J. Am. Soc. Nephrol. 19 (9), 1653–1658.

Gavrilovskaya, I.N., Brown, E.J., Ginsberg, M.H., Mackow, E.R., 1999. Cellular entry of hantaviruses which cause hemorrhagic fever with renal syndrome is mediated by beta3 integrins. J. Virol. 73 (5), 3951–3959.

Geimonen, E., Neff, S., Raymond, T., Kocer, S.S., Gavrilovskaya, I.N., Mackow, E.R., 2002. Pathogenic and nonpathogenic hantaviruses differentially regulate endothelial cell responses. Proc. Natl. Acad. Sci. U. S. A. 99 (21), 13837–13842.

Guhl, S., Franke, R., Schielke, A., Johne, R., Krüger, D.H., Babina, M., Rang, A., 2010. Infection of in vivo differentiated human mast cells with hantaviruses. J. Gen. Virol. 91 (Pt 5), 1256–1261.

Hepojoki, J., Strandin, T., Wang, H., Vapalahti, O., Vaheri, A., Lankinen, H., 2010. Cytoplasmic tails of hantavirus glycoproteins interact with the nucleocapsid protein. J. Gen. Virol. 91 (Pt 9), 2341–2350.

Higa, M.M., Petersen, J., Hooper, J., Doms, R.W., 2012. Efficient production of Hantaan and Puumala pseudovirions for viral tropism and neutralization studies. Virology 423 (2), 134–142.

Korva, M., Saksida, A., Kejzar, N., Schmaljohn, C., Avsic-Zupanc, T., 2013. Viral load and immune response dynamics in patients with haemorrhagic fever with renal syndrome. Clin. Microbiol. Infect. 19 (8), E358–366.

Krautkrämer, E., Grouls, S., Stein, N., Reiser, J., Zeier, M., 2011. Pathogenic old world hantaviruses infect renal glomerular and tubular cells and induce disassembling of cell-to-cell contacts. J. Virol. 85 (19), 9811–9823.

Krautkrämer, E., Zeier, M., 2008. Hantavirus causing hemorrhagic fever with renal syndrome enters from the apical surface and requires decay-accelerating factor (DAF/CD55). J. Virol. 82 (9), 4257–4264.

Krautkrämer, E., Zeier, M., 2014. Old World hantaviruses: aspects of pathogenesis and clinical course of acute renal failure. Virus Res. 187, 59–64.

Li, J., Zhang, Q., Wang, T., Li, C., Liang, M., Li, D., 2010. Tracking hantavirus nucleocapsid protein using intracellular antibodies. Virol. J. 7, 339.

Lundkvist, A., Cheng, Y., Sjolander, K.B., Niklasson, B., Vaheri, A., Plyusnin, A., 1997. Cell culture adaptation of Puumala hantavirus changes the infectivity for its natural reservoir, Clethrionomys glareolus, and leads to accumulation of mutants with altered genomic RNA S segment. J. Virol. 71 (12), 9515–9523.

Mantula, P.S., Outinen, T.K., Clement, J.P.G., Huhtala, H.S.A., Porsti, I.H., Vaheri, A., Mustonen, J.T., Makela, S.M., 2017. Glomerular Proteinuria Predicts the Severity of Acute Kidney Injury in Puumala Hantavirus-Induced Tubulointerstitial Nephritis. Nephron 136 (3), 193–201.

Mustonen, J., Helin, H., Pietila, K., Brummer-Korvenkontio, M., Hedman, K., Vaheri, A., Pasternack, A., 1994. Renal biopsy findings and clinicopathologic correlations in nephropathia epidemica. Clin. Nephrol. 41 (3), 121–126.

Nemirov, K., Lundkvist, A., Vaheri, A., Plyusnin, A., 2003. Adaptation of Puumala hantavirus to cell culture is associated with point mutations in the coding region of the L segment and in the noncoding regions of the S segment. J. Virol. 77 (16), 8793–8800.

Prescott, J., Feldmann, H., Safronetz, D., 2017. Amending Koch's postulates for viral disease: when "growth in pure culture" leads to a loss of virulence. Antiviral Res. 137, 1–5.

Ramanathan, H.N., Jonsson, C.B., 2008. New and Old World hantaviruses differentially utilize host cytoskeletal components during their life cycles. Virology 374 (1), 138–150.

Reuter, M., Krüger, D.H., 2018. The nucleocapsid protein of hantaviruses: much more than a genome-wrapping protein. Virus Genes 54 (1), 5–16.

Saksida, A., Duh, D., Korva, M., Avsic-Zupanc, T., 2008. Dobrava virus RNA load in patients who have hemorrhagic fever with renal syndrome. J. Infect. Dis. 197 (5), 681–685.

Saleem, M.A., O'Hare, M.J., Reiser, J., Coward, R.J., Inward, C.D., Farren, T., Xing, C.Y., Ni, L., Mathieson, P.W., Mundel, P., 2002. A conditionally immortalized human podocyte cell line demonstrating nephrin and podocin expression. J. Am. Soc. Nephrol. 13 (3), 630–638.

Shimizu, K., Yoshimatsu, K., Koma, T., Yasuda, S.P., Arikawa, J., 2013. Role of nucleocapsid protein of hantaviruses in intracellular traffic of viral glycoproteins. Virus Res. 178 (2), 349–356.

Shin, O.S., Kumar, M., Yanagihara, R., Song, J.W., 2013. Hantaviruses induce cell type- and viral species-specific host microRNA expression signatures. Virology 446 (1-2), 217–224.

Temonen, M., Vapalahti, O., Holthofer, H., Brummer-Korvenkontio, M., Vaheri, A., Lankinen, H., 1993. Susceptibility of human cells to Puumala virus infection. J. Gen. Virol. 74 (Pt 3), 515–518.

Vaheri, A., Strandin, T., Hepojoki, J., Sironen, T., Henttonen, H., Makela, S., Mustonen, J., 2013. Uncovering the mysteries of hantavirus infections. Nat. Rev. Microbiol. 11 (8), 539–550.

Welsh, G.I., Saleem, M.A., 2011. The podocyte cytoskeleton–key to a functioning glomerulus in health and disease. Nat. Rev. Nephrol. 8 (1), 14–21.

Witkowski, P.T., Bourquain, D., Bankov, K., Auste, B., Dabrowski, P.W., Nitsche, A., Krüger, D.H., Schaade, L., 2016. Infection of human airway epithelial cells by different subtypes of Dobrava-Belgrade virus reveals gene expression patterns corresponding to their virulence potential. Virology 493, 189–201.

Yi, J., Xu, Z., Zhuang, R., Wang, J., Zhang, Y., Ma, Y., Liu, B., Zhang, C., Yan, G., Zhang, F., Yang, A., Jin, B., 2013. Hantaan virus RNA load in patients having hemorrhagic fever with renal syndrome: correlation with disease severity. J. Infect. Dis. 207 (9), 1457–1461.